Dual-Satellite Formation Flying Demonstration in Near Circle Orbit[1]

Shengchao DENG, Tao MENG, Zhonghe JIN
Microsat Research Center, Zhejiang University
NO.38, Zheda Road, Hangzhou, P.R.China, 310027
Email: dscsd.0131@gmail.com

Abstract: After two years successful in-orbit operation of ZDPS-1A satellite, Zhejiang University is planning to design a dual-satellite platform, ZDPS-2, for formation flying demonstration. The platform consists of two nano-satellites, both are 25 × 25 × 25 cm3 cube-shaped and weigh around 12kg, planned for launch before the middle of 2014 and their designed life time is 3 years. The major purposes of this mission are the validation of MEMS accelerometer in-orbit calibration, Pseudo-Noise code ranging system, micro-propulsion system as well as formation control technology. The formation control modes include ground-based formation flying and fully autonomous formation flying. Both satellites will carry a cold gas propulsion system, which allows exchanging roles to perform additional experiments. It utilizes ammonia as propellant, capable of delivering thrust (30mN) along tracking and normal direction with a total delta-V of about 24 m/s. Furthermore, multi-directional observation will be investigated as the secondary mission. The paper gives a brief introduction of Dual-Satellite platform and the related formation experiments to be demonstrated on orbit. The thruster design and formation control algorithm will be detailed presented with numerical simulation verification.

Keywords: *ZDPS-2, Formation Flying, Propulsion, LQR*

1. Introduction

Nowadays, nanosatellites play a more important role in scientific and commercial applications, including new technology experiments, wireless communications, space observations, etc. With increasing demand in distributed detection and in-orbit service, multi-satellite system is identified as the next revolutionary step in development of space technology. SNAP-1[1], designed by SSTL&SSC and launched in 2000, demonstrated a propulsion system and formation flying with Tsinghua-1. In 2006, three space technology-5 (ST-5)[2] satellites developed by NASA successfully formed a space constellation to execute the observation of geomagnetic field. The PRISMA test bed[3] built by SSC was launched in 2010 and actualized autonomous formation flying, homing & rendezvous scenarios, as well as close-range proximity operations.

However, much of the research has centered on formation flying while few projects have been designed and accomplished successfully. In this framework, ZDPS-2, a dual-satellite platform mission is designed by Zhejiang University to provide a technology demonstration of guidance, navigation and control (GNC) strategies for spacecraft formation flying. This paper describes the ZDPS-2 design scheme, especially the propulsion system. Then, algorithms for formation flying and several numerical simulations are presented.

[1] Supported by “the Fundamental Research Funds for the Central Universities”

2. ZDPS-2 Mission

ZDPS-2 is the latest Nano-satellite mission of Microsat Research Center, Zhejiang University. It constitutes an in-orbit test platform for formation flying technology with two identical nano-satellites, ZDPS-2A and ZDPS-2B. The main objectives of ZDPS-2 mission are as follows.

- Demonstrate advanced guidance, navigation and control algorithms for formation flying.
- In-orbit performance test of self-designed ammonia micro-propulsion system.
- Validate the precision of the S-Band Inter-Satellite Pseudo-Noise(PN) code ranging system.
- Validate the dual-frequency GPS receiver and the relative orbit determination algorithm.
- Validate the MEMS accelerometer in-orbit calibration algorithm.

The main subsystems and components of the ZDPS-2 gained space heritage on the ZDPS-1A mission[4]. ZDPS-1A01&02 are the first pico-satellites that have been launched successfully in China, which are both 15 × 15 × 15 cm3 cube-shaped with a total mass of 3.5kg. They were delivered by a Long-March-2D (CZ-2D) rocket and launched into a sun-synchronous orbit on Sept 22nd, 2010. After two years successful in-orbit operation, main components of ZDPS-1A still work well. These provide a reliable guarantee for the design of ZDPS-2 and the further formation experiments.

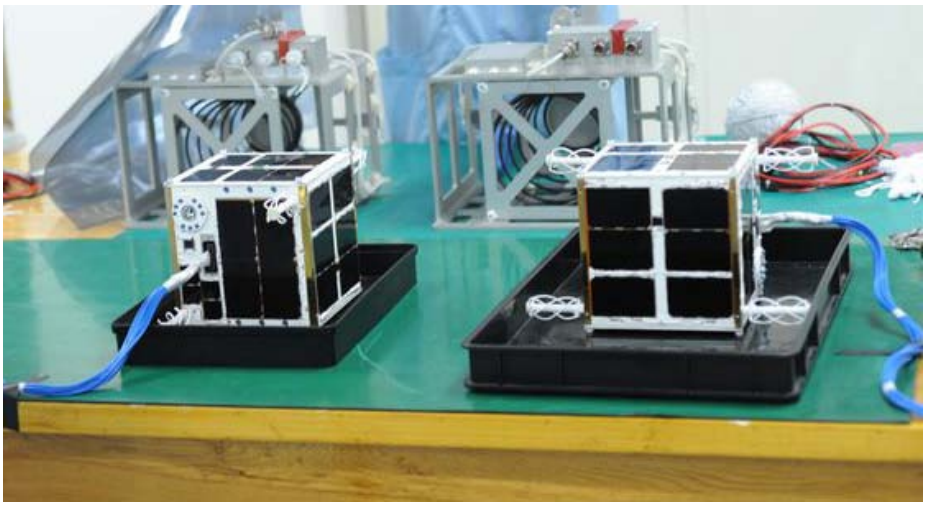

Figure 1. View of the integrated ZDPS-1A Satellites with its disengaging gear

Both ZDPS-2A and ZDPS-2B are 25 × 25 × 25 cm3 cube-shaped and weigh around 12kg. The satellites are equipped with tri-junction Ga-As solar cells as the primary power, tiled on all six planes of the satellite body, which have a 26.8% theoretical efficiency, and a Li-ion battery pack of ten cells from Sanyo serves as the secondary power[5]. The transceiver works under the Universal S-Band (USB) TTC system[6][7], enjoys uplink data rates of 2kbps and adjustable downlink data rates of

1kbps-64kbps. The on-board computer(OBC) is composed of multi-CPU with FPGA, providing a universal computing, storage, management platform for command execution, TT&C, attitude & orbit control, payloads, etc.

Sub-degree level attitude measurement will be achieved through a 3-axis magnetometer[8], a 3-axis MEMS gyroscope, four-quadrant analog sun sensors[9] mounted on six surfaces and a digital sun sensor[10][11]. Attitude control utilizes a momentum wheel, installed on the pitch axis, to provide both momentum bias and reaction actuation for pitch attitude maneuver, and three orthogonally mounted magnetic coils provide active control torque for detumbling and three-axis stabilization, with pointing accuracy of better than 2° and steady precision 0.1°/s.

In order to obtain an accurate absolute position and velocity measurement, ZDPS-2 carries two GPS receivers. A UNICORE dual-frequency GPS receiver provides single-point positioning accuracy of 2m (RMS), with observational data updating rate up to 10Hz. A Zhejiang University developed GPS receiver provides absolute position accuracy of 2m and velocity of 0.2m/s. A dual-frequency GPS antenna is mounted on the face opposite to the ground (-Z plane).

ZDPS-2A&B are each equipped with an S-Band inter-satellite communication transceiver to exchange position and velocity data, capable of providing data transmission rate of 8kbps and maximum communication range of 5km. In addition, an S-Band PN code ranging system is designed to provide PN code rate of no more than 2Mcps, and ranging accuracy of 4cm for 1Mcps code rate. It could support for multiple composite codes such as JPL1999, T2, T4 and so on.

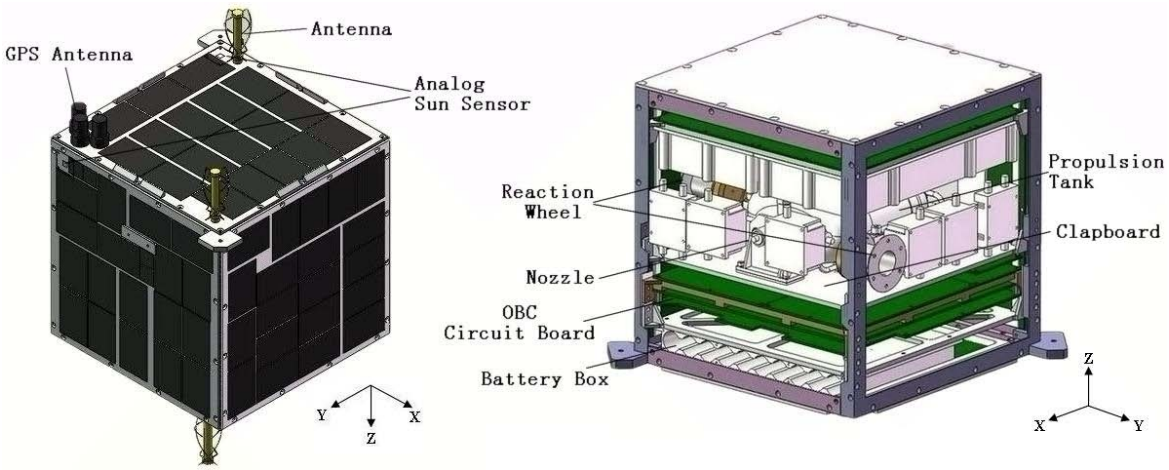

Figure 2. View of the external (left) and internal (right) ZDPS-2 Structure

3. Propulsion System

ZDPS-2A&B are both equipped with propulsion system, either of them can be treated as chief or deputy. The system uses liquid ammonia as a propellant with ISP greater than 900Ns/kg. With the fuel mass of 0.318kg and the satellite mass of below 12kg, the system can provide a total ΔV of 24m/s. The performance of ZDPS-2 propulsion system is as follows.

Table 1. Propulsion System Performance

Component	Requiement
Propellant	liquid ammonia
Tank volume	0.6L
Thruster Number	Four(±X,±Y)
Operating Pressure	0.15~2.4MPa
Operating Temperature	-10°C～+45°C
Switching Delay Time	Turn on: 3.5ms Turn off: 2ms
Rated Thrust Magnitude	30mN@0.8MPa&20°C
Rated Isp	≥900Ns/kg@0.8MPa&20°C
Power	1W@12VDC
Total Leak Rate	≤1×10-4 Pa·m^3/s

3.1. System Structure

Four thrusters are mounted along the ±X and ±Y direction through the centroid of satellite as shown in Fig.2. A propulsion tank of 0.6L is used for storing liquid ammonia. Saturated ammonia vapor spurts out through the pipe when the thruster is turned on, then generates a thrust and provides required impulse. To ensure the accuracy of the thrust, the minimum impulse time is set to 10ms due to the thruster switching delay. And the designed maximum opening time is limited to 50s to avoid the nozzle frozen by injection.

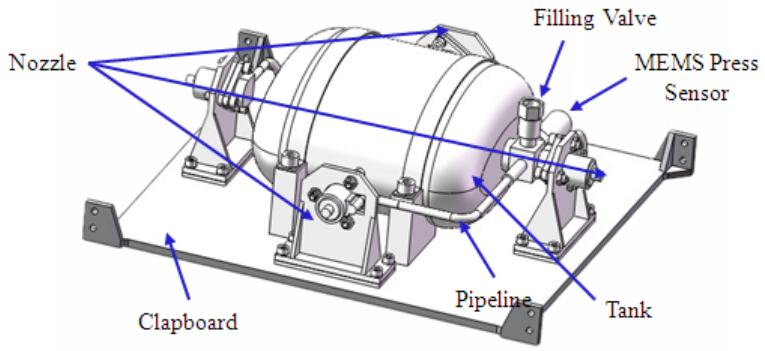

Figure 3. ZDPS-2 Ammonia Propulsion System Structure

MEMS pressure sensor and temperature sensor are selected to monitor the system operating condition. Three orthogonally mounted MEMS accelerometers are used to calculate the actual thrust. Heating resistance wire is winded around the pipe to ensure the liquid ammonia get adequate gasification. Controlling PCB is mounted on the back of the clapboard to shorten the electrical circuit.

3.2. PWM Method

As ZDPS-2 propulsion system provides 30mN constant thrust, it requires PWM strategy to meet the maneuver needs, viz., the thruster on time (Ton) is varied. At the beginning of each PWM period, the open thruster No. is determined by the thrust direction, and the on time is computed as

$$T_{on} = \min(\frac{|u|}{U_{const}}, T_{\max}) \quad (1)$$

where |u| is the theoretical value of the thrust, U_{const} denotes the constant thrust, T_{max} is the system allowed maximum on time. Once finish the compute, OBC sends the thruster No. and T_{on} to the actuator to turn on/off the thrust.

The selection of T_{PWM} influences the feedback control precision a lot. Short cycle will cause the thrust frequency on-off, and long cycle results in unstable control. We select 120s as PWM control cycle according to the comprehensive consideration of the simulation and ground experiments.

3.3. Thruster Turnoff Mode

In order to verify the MEMS accelerometer in-orbit performance, two control mode of thruster turnoff have been designed. Formation algorithms figure out the required ΔV or the thruster on time, one mode turns off the thruster when the accelerometers outputs integral accumulation is equal to ΔV, and the other determines the off time directly by the MCU timer.

To reduce the influence of gravitational perturbing acceleration, attitude slowly disturbance and accelerometer zero-drift error, the integral method is set as follows:

1. No thrust actuated: integral accumulate the outputs by a certain frequency; set the average as the disturbance mean value, and refresh periodically.

2. Thrust open: accumulate the outputs at the beginning of the thrust; each sampling point subtracts the disturbance mean value as the actual thrust acceleration, and turn off when it is equal to ΔV.

4. Formation Flying Experiment

4.1. Formation Mission

The designed orbit of ZDPS-2A&B is a 700km sun-synchronous orbit. Considering the future aviation application requirements and the ZDPS-2 payload constraints, we have designed a two stage experiment. The first stage includes the ordinary in-plane track formation and the circular formation[12]. Each configuration will be maintained for about 30 orbits (two days). In the in-plane along track formation, the chief and deputy occupy the same orbital plane, but are separated by mean anomaly. The circular formation is one in which satellites maintain a constant distance from each other. When one formation is completed, the next will be reached according to the ground instruction.

A fixed configuration formation is suitable for long-term tracking of the chief, but the observation angle and orientation is single. Natural orbit multi-directional observation can be achieved by continuously modifying the reference configuration. So when the above plan has been executed successfully, the experiment will enter the secondary stage, which includes elliptical and spiral formation observation. Elliptical formation

observes the target satellite by continually changing the relative motion phase difference of orbital plane and orbital normal axis. The basic configuration of spiral formation is also an elliptical. The deputy satellite will have a velocity direction procession through an impulse thrust, then form a spiral and deploy the observation.

After deployed from the launch vehicle, ZDPS-2A&B are assumed to be at the same position. The deputy satellite performs approximately 56.28mm/s ΔV along the anti-velocity direction, two satellites will start to separate. After drifting for two orbits, the deputy will perform another thrust to halt the separation and come into a 2km in-plane track formation. Then a 1km in-plane track, a 500m circular formation, a 100m circular formation will perform in sequence. During the second stage demonstration, two satellites will change roles, in order to balance the fuel consumption.

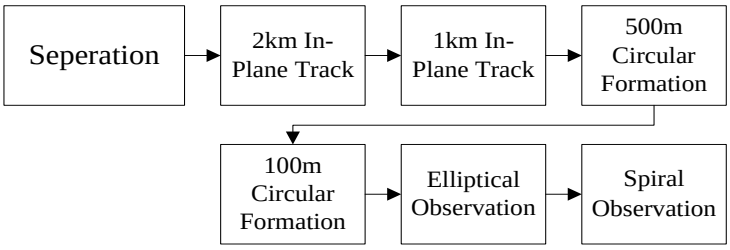

Figure 4. Entire ZDPS-2 Formation Demonstration Procedure

In order to guarantee the implementation of the orbital maneuver and append additional experiments, ZDPS-2 applies two types of control mode: ground-based control and automatic formation control. In the former mode, the ground station calculates the control sequence according to different missions and switches the thrusters by sending telecontrol instructions, but the actual thrust magnitude is hard to accurately predict. In the latter mode, the satellite uses OBC system to run the formation algorithm through real-time ISL and ranging measurement information, so the thruster error could be compensated by closed-loop feedback control and achieve a high precision formation networking.

4.2 Formation Algorithm

4.2.1 Orbit Propagation

According to the orbital dynamics equation, orbital motion of the two satellites in the GCI coordinate system can be evolved by the formula:

$$\begin{aligned} \ddot{\mathbf{r}}_c &= -\frac{\mu \mathbf{r}_c}{r_c^3} + \mathbf{f}_c \\ \ddot{\mathbf{r}}_d &= -\frac{\mu \mathbf{r}_d}{r_d^3} + \mathbf{f}_d + \frac{\mathbf{F}_d}{m_d} \end{aligned} \tag{2}$$

where: μ for the Earth's gravitational constant; $\mathbf{f}_c$ and $\mathbf{f}_d$ denote the perturbation acceleration acting on the chief and the deputy satellite; $\mathbf{F}_d$ for the control force applied to the deputy; m_d for the mass of the deputy.

For a 700km sun-synchronous orbit and a 12kg weight, 25cm cube-shaped satellite, the acceleration magnitude of J2 perturbation effect is about 0.02 m/s^2, while the

atmospheric drag is 1.8e-7 m/s^2, much less than the former. The differential drag influence can be ignored when calculating the relative motion, as ZDPS-2A&B have nearly the same mass-area ratio. So only the J2 perturbation is considered in the orbital propagator. OBC utilizes an 4th Runge-Kutta method to do the numerical integration, and refreshes initial values by GPS data or ground station data regularly.

In addition, OBC calculates the relative position and velocity in the GCI frame through ISL data.

$$\begin{aligned}\mathbf{X}_I &= \mathbf{r}_d - \mathbf{r}_c = [x, y, z]^T \\ \mathbf{V}_I &= \dot{\mathbf{r}}_d - \dot{\mathbf{r}}_c = [\dot{x}, \dot{y}, \dot{z}]^T\end{aligned} \tag{3}$$

Then transform these two vectors into the Hill frame, which moves with the chief. Its x-axis is in the orbit radial direction, y-axis in the orbital velocity direction and z-axis completes the right-handed coordinate system. The transfer matrix is

$$\begin{aligned}\mathbf{X}_H &= \mathbf{A}_{hi}\mathbf{X}_I, \mathbf{A}_{hi} = \left[\frac{\mathbf{r}_c}{|\mathbf{r}_c|} \quad \frac{\mathbf{H}_c \times \mathbf{r}_c}{|\mathbf{H}_c \times \mathbf{r}_c|} \quad \frac{\mathbf{H}_c}{|\mathbf{H}_c|}\right]^T \\ \mathbf{V}_H &= \mathbf{A}_{hi}\mathbf{V}_I - \omega \times \mathbf{X}_H\end{aligned} \tag{4}$$

where $\mathbf{H}_c$ is for the orbital angular momentum of the chief; $\boldsymbol{\omega} = [0,0,n]^T$ denotes the orbital angular rate of the chief in the orbit coordinate.

During the Formation Keeping mode, control algorithm yields periodic relative motion based on a series of preset reference trajectories and closely meets the natural orbital motion. We use the CW equations[14] to describe the reference trajectory. They linearize the nonlinear and nonperiodic relative motion and assume that eccentricity of the chief orbit is close to 0.

$$\begin{cases}\ddot{x} - 2n\dot{y} - 3n^2 x = 0 \\ \ddot{y} + 2n\dot{x} = 0 \\ \ddot{z} + n^2 z = 0\end{cases} \tag{5}$$

Where $n = \sqrt{\mu / a^3}$ is the circular orbital rate. When calculating the circular formation reference trajectory, first get the initial relative motion vector in the Hill frame from the initial target orbit, then propagate above equations through 4th Runge-Kutta integration and refresh periodically. When it comes to in-plane track, (0,l,0) is used as the reference trajectory directly.

4.2.2 Formation orbit design

Design of the deputy orbit will be in accordance with five formation configuration elements (p,s,α,θ,l), defined as follows[13]:

1. p: semiminor axis of the projection ellipse in the x-y plane (orbital plane). If p = 0, the relative motion degenerate to the simple harmonic oscillation in the z-direction.
2. s: amplitude of the z-direction (orbital normal axis) simple harmonic oscillation. If s = 0, the relative motion is an ellipse in the x-y plane, with the ratio of the major-minor axis is 2:1.
3. α: relative motion initial phase difference of x-y plane and z-direction.
4. θ: relative motion initial phase of x-y plane.

5. l: distance between the formation center and the chief. If l> 0, the formation center is in front of the chief and vice versa.

The relative motion equation expressed by the five elements is

$$\begin{aligned} x &= -p\cos(nt+\theta) \\ y &= 2p\sin(nt+\theta)+l \\ z &= s\sin(nt+\theta-\alpha) \end{aligned} \tag{6}$$

Table.2 are the first stage configuration parameters according to the designed demonstration scheme.

Table 2. First Stage Demonstration Configuration Parameters

	p/km	s/km	α/rad	θ/rad	l/km
2km In-Plane	0	0	0	0	2
1km In-Plane	0	0	0	0	1
500m Circular	0.25	0.433	π/2	0	0
100m Circular	0.05	0.0866	π/2	0	0

When it comes to the secondary stage, for the elliptical observation, first set the reference configuration to a 50m circular formation, then change the differential initial phase α from 0 to 2π at π/3 interval, with each phase for one orbit. Phase modification algorithm is LQR feedback method, homology as the formation-keeping which will go into particulars later. This will lead to an all-around observation expect for the narrow orbit normal visual angle.

Natural spiral formation essentially is an ellipse with an out-of-plane motion. The central axis is parallel to the y-axis. In addition to the five elements of the general conformation, spiral-shaped parameters h denotes the screw pitch that determines the level of drift distance during one orbit time. The formation can be achieved through a y-direction impulse at the intersection of the tilting ellipse and the in-plane straight line $y=y_s$, where y_s is the initial position of the formation. The algorithm is $\Delta V_t = h \cdot n / 2\pi$.

After accomplishing the elliptical observation, first modify the configuration to a 50m circular formation with differential initial phase θ=π, then apply a tangential thrust when y-direction distance is 50m. Here the deputy will gradually fall behind the chief. After 5 orbits, apply a double thrust on the –y-axis to achieve reverse drift, At last, apply a thrust to hold the drift when the deputy is back to the ellipse center.

4.2.3 Seperation&Reconfiguration Control Law

For the in-plane track→in-plane track reconfiguration, only the center distance l among the formation elements requires modification[16]. If the thrust size doesn't satisfy, the reconfiguration can last several orbits.

Table 3. In-Plane Track Reconfiguration Scheme

Component	first impulse	second impulse
Location	f=0	f=0
Radial	0	0

Tangential	$-\frac{1}{6N\pi}n\Delta l$	$\frac{1}{6N\pi}n\Delta l$
Normal	0	0

Where f is the true anomaly of the deputy; N is the orbit number between two impulses. $\Delta l = l_2 - l_1$ is the distance difference between two configurations.

For the in-plane track→circular formation & circular →circular formation, we use the nonsingular orbit elements **e** = [a,q_1,q_2,I,Ω,λ], where $q_1 = e\cos\omega$, $q_2 = e\sin\omega$, $\lambda = \omega + M$. Relation between the impulse thrust and relative elements in the Hill frame can be derived from the Gauss perturbation equation in terms of nonsingular elements. For the near circle orbit,

$$\begin{aligned}
&\delta i \approx \gamma \cos u \Delta V_h \\
&\delta\Omega \approx (\gamma \sin u / \sin i)\Delta V_h \\
&\delta a \approx (2/n)\Delta V_t \\
&\delta q_1 \approx \gamma \sin u \Delta V_r + 2\gamma \cos u \Delta V_t \\
&\delta q_2 \approx -\gamma \cos u \Delta V_r + 2\gamma \sin u \Delta V_t \\
&\delta\lambda \approx -2\gamma\Delta V_r - \gamma \sin u \cot i \Delta V_h
\end{aligned} \tag{7}$$

where $\gamma = \sqrt{a/\mu}$, $(\Delta V_r, \Delta V_t, \Delta V_h)$ is the impulse thrust along the radial, tangential and orbital normal direction.

Assuming initial phase difference of the configuration between in-plane and out-of-plane is 0, distance between the configuration center and the chief is 0, formation elements before and after the reconfiguration is (p_1,s_1,π/2,θ_1,l_1) and (p_2,s_2,π/2,θ_2,l_2), then the desired deputy orbit elements difference can be written as Eq.8

$$\begin{aligned}
&\delta a = 0 \\
&\delta q_1 = -\frac{p_2}{a}\sin\theta_2 + \frac{p_1}{a}\sin\theta_1 \\
&\delta q_2 = -\frac{p_2}{a}\cos\theta_2 + \frac{p_1}{a}\cos\theta_1 \\
&\delta i = \frac{s_2}{a}\cos\theta_2 - \frac{s_1}{a}\cos\theta_1 \\
&\delta\Omega = \frac{s_2}{a}\frac{\sin\theta_2}{\sin i} - \frac{s_1}{a}\frac{\sin\theta_1}{\sin i} \\
&\delta\lambda = -\delta\Omega\cos i
\end{aligned} \tag{8}$$

The impulse thrust will be calculated as Table.4.

Table 4. Circular Formation Reconfiguration Scheme

Component	first impulse	second impulse
Location	$u = u_o$	$u = u_o + \pi$
Radial	$-\frac{\sqrt{\delta q_1^2 + \delta q_2^2}}{2\gamma}$	$\frac{\sqrt{\delta q_1^2 + \delta q_2^2}}{2\gamma}$

Tangential	0	0
Normal	$\frac{\sqrt{\delta i^2 + \delta\Omega^2 \sin^2 i}}{\gamma}$	0

Where u = ω+f is the argument of latitude of the deputy, and $u_o = 2\pi - \tan^{-1}(\delta q_1 / \delta q_2)$, $\gamma = \sqrt{a/\mu}$.

Due to the lack of radial thrust on ZDPS-2A&B, attitude should be adjusted in time as this scheme. For reducing the attitude control complexity, and ignoring the requirement of formation initial phase, we can combine the tangential impulse scheme in in-plane track→ in-plane track reconfiguration and normal impulse scheme in this section. If $\theta_1 = \theta_2 = 0$, then $\delta i = (s2 - s1)/a, \delta\Omega = 0, \sqrt{\delta i^2 + \delta\Omega^2 \sin^2 i}/\gamma = \Delta s / a\gamma = n\Delta s$. Details are as the Table.5.

Table 5. In-plane Track & Circular Formation Reconfiguration Scheme

Component	first impulse	second impulse	third impulse	fourth impulse
Location	f=0	f=π/2	f=π	f=2π
Radial	0	0	0	0
Tangential	$\frac{1}{16}n(2\Delta p) - \frac{1}{6\pi}n\Delta l$	0	$-\frac{1}{8}n(2\Delta p)$	$\frac{1}{16}n(2\Delta p) + \frac{1}{6\pi}n\Delta l$
Normal	0	$n\Delta s$	0	0

4.2.4 Formation Keeping Feedback Control Law

The relative error dynamics can be expressed in state space form:

$$\dot{\tilde{\mathbf{x}}} = \mathbf{A}\tilde{\mathbf{x}} + \mathbf{B}\mathbf{u} \tag{9}$$

where $\tilde{\mathbf{x}}$ for the relative state error vector and **u** for the control vector.

$$\begin{aligned} \tilde{\mathbf{x}} &= \mathbf{x}_d - \mathbf{x}_{ref} = [x, y, z, \dot{x}, \dot{y}, \dot{z}]^T \\ \mathbf{u} &= [u_x, u_y, u_z]^T \end{aligned} \tag{10}$$

According to the CW equations, the state error matrix **A** is

$$\mathbf{A} = \begin{bmatrix} & 0_{3\times3} & & & I_{3\times3} & \\ & & & & & \\ 0 & 0 & 0 & 0 & 2n & 0 \\ 3n^2 & 0 & 0 & -2n & 0 & 0 \\ 0 & 0 & -n^2 & 0 & 0 & 0 \end{bmatrix} \tag{11}$$

and as only four faces are equipped with thruster on ZDPS-2, the control matrix **B** is set as

$$\mathbf{B} = \begin{bmatrix} 0_{3\times3} \\ I_{3\times3} - \mathrm{diag}([1,0,0]) \end{bmatrix} \tag{12}$$

relative motion in the x-y plane is mutual coupling, so we can reach the similar control result only by thrusts on velocity direction. Then a Linear Quadratic Regulator (LQR) method is used to find the optimized control output u so that the quadratic cost function

$$J = \int_0^\infty (\tilde{\mathbf{x}}^T \mathbf{Q} \tilde{\mathbf{x}} + \mathbf{u}^T \mathbf{R} \mathbf{u}) dt \tag{13}$$

is minimized for a give $\tilde{\mathbf{x}}$. **Q** and **R** are the state cost matrix and the input cost matrix respectively, and can measure the magnitude of the error in the control process and the total control consumption. **Q** and **R** are set as follows by the simulation verification and can be modified by the ground data injection.

$$\mathbf{Q} = 0.8 \cdot \begin{bmatrix} 10^{-6} \cdot I_{3\times3} & 0_{3\times3} \\ 0_{3\times3} & I_{3\times3} \end{bmatrix}, \mathbf{R} = 10^4 \cdot I_{3\times3} \tag{14}$$

Then we get the optimal feedback control input

$$\mathbf{u} = -\mathbf{R}^{-1}\mathbf{B}^T \mathbf{P} \tilde{\mathbf{x}} \tag{15}$$

where **P** is the solution of the algebraic Riccati equation:

$$\mathbf{A}_h^T + \mathbf{P}\mathbf{A}_h - \mathbf{P}\mathbf{B}\mathbf{R}^{-1}\mathbf{B}^T\mathbf{P} + \mathbf{Q} = \mathbf{0} \tag{16}$$

5. Simulation Results

The entire ZDPS-2 formation demonstration procedure was simulated and the results are presented as follows.

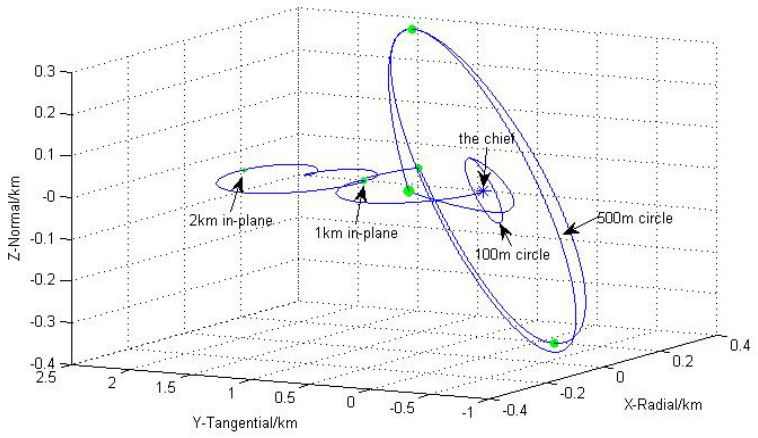

Figure 5. Relative Motion of ZDPS-2 First Stage Demonstration

Figure.5 illustrates the relative motion of the first stage in the Hill coordinate system, the deputy form the configuration as the preset sequence: 2km in-plane → 1km in-plane → 500m circular → 100m circular.

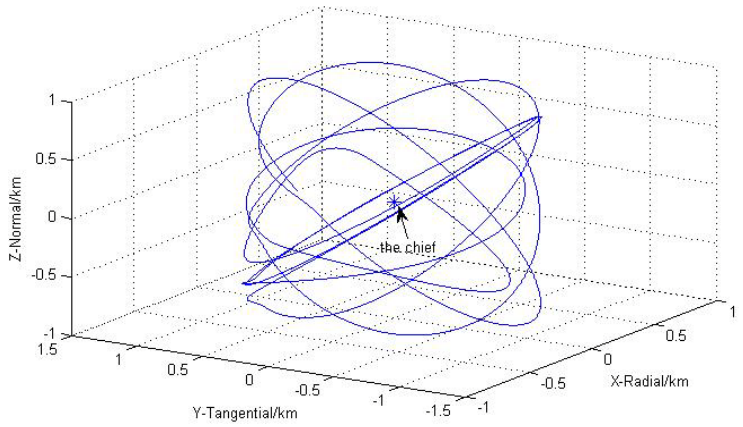

Figure 6. Relative Motion of ZDPS-2 Elliptical Observation

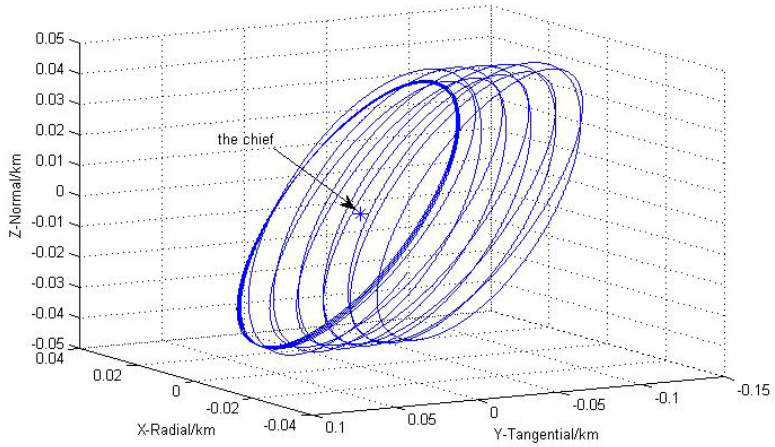

Figure 7. Relative Motion of ZDPS-2 Spiral Observation

Figure.6&7 illustrates the relative motion of the elliptical and the spiral observation respectively. The deputy can observe the chief from multi-angle. After each observation, the deputy will fly around the chief according to a certain formation.

The simulation shows that the tracking error <4.12m (RMS) for the 2km in-plane track and <0.93m (RMS) for the 100m circular formation, and meets well the mission requirements under this propulsion capability and GPS measurement accuracy. Maintenance and reconfiguration of the first stage is expected to require 1.34m/s ΔV, and the second stage requires 0.19m/s ΔV, which well beneath the 24m/s available on each satellite. On this basis, the ground station could design more experiments for the ZDPS-2 platform.

Table 6. Fuel Consumption of Reconfiguration

Formation	ΔV(m/s)
Initial Separation	0.1126
2km→1km In-Plane	0.0563
1km In-Plane	0.0118

1km In-Plane→500m Circular	0.6396
500m→100m Circular	0.4747
100m→50m Circular	0.0593
Elliptical Observation	0.1301
Spiral Observation	0.0035

Table 7. Fuel Consumption of Formation-keeping and Tracking Error

Formation	ΔV(m/s)	tracking error(m)
2km In-Plane	0.0099	4.1198
1km In-Plane	0.0118	1.8645
500m Circular	0.0154	1.0473
100m Circular	0.0182	0.9223

6. Conclusion

ZDPS-2 is a dual-satellite formation flying demonstration platform in near circle orbit, which will validate several key technologies, including formation flying control, multiple Band transceivers and GPS receivers. This paper introduces the mission and the primary technologies, and mainly discusses the formation flying algorithm.

Formation algorithm utilizes impulsive control based on mean orbit elements to implement the formation reconfiguration, and LQR state-feedback control law to keep the current formation. PWM method with a period of 120s was designed to adapt to the constant 30mN force from thrusters. MEMS accelerometers' outputs will be calculated to confirm the turnoff of the thrusters. Numerical simulations of the overall mission indicate the tracking error is below 1.8m (RMS) and the total ΔV of two stages is approximately 1.53 m/s.

So far, ZDPS-2 mission have finished the subsystem prototype design, and the next will come into the engineering model design and reliability verification, ground testes, including hardware-in-the-loop simulations. ZDPS-2A&B are expected to be launched before the middle of 2014.

7. References

[1] Underwood C I, Richardson G, Savignol J. In-orbit results from the SNAP-1 nanosatellite and its future potential[J]. Philosophical Transactions of the Royal Society of London. Series A: Mathematical, Physical and Engineering Sciences, 2003, 361(1802): 199-203.

[2] Carlisle C C, Finnegan E J. Space Technology 5: pathfinder for future micro-sat constellations[C]//Aerospace Conference, 2004. Proceedings. 2004 IEEE. IEEE, 2004, 1.

[3] Gill E, Montenbruck O, D'Amico S. Autonomous formation flying for the PRISMA mission[J]. Journal of Spacecraft and Rockets, 2007, 44(3): 671-681.

[4] YANG Mu, WANG Hao, WU Changju, WANG Chunhui, DING Licong , ZHENG

Yangming, JIN Zhonghe. Space Flight Validation of Design and Engineering of the ZDPS-1A Pico-satellite[J]. Chinese Journal of Aeronautics, 2012, (05):725-738.

[5] DING Licong, JIN Xiaojun, WANG Chunhui, JIN Zhonghe. Design and on-orbit verification of ZDPS-1A power system[J]. Journal of Zhejiang University (Science A: An International Applied Physics & Engineering Journal), 2013

[6] YUAN Tieshan, ZHANG Chaojie, YANG Weijun, JIN Zhonghe. Implementation of a New S-Band Micro-Transponder Based on Software Defined Radio[J]. Chinese Journal of Sensors and Actuators, 2012,(06):756-760.

[7] ZHOU Yang, WANG Chunhui, JlN Xiaojun, JIN Zhonghe. A New Receiver Structure of TT&C Transponder for Pico-Satellite[J]. Chinese Journal of Sensors and Actuators, 2011,(05):694-699.

[8] CAI Bo, WANG Hao, ZHU Xiaofeng, HAN Ke, JIN Zhonghe. Design of the Earth Magnetic Field Measurement System for Pico-Satellites[J]. Chinese Journal of Sensors and Actuators, 2011,(08)

[9] WANG Jun, WANG Hao, YING Peng, JIN Zhonghe. Design of Four-Quadrant Analog Sun Sensor[J]. Chinese Journal of Sensors and Actuators, 2012(12)

[10] HAN Ke, WANG Hao, TU Binjie, JIN Zhonghe Department of Information Science and Electronic Engineering, Zhejiang University, Hangzhou 310027, China. Pico-satellite Autonomous Navigation with Magnetometer and Sun Sensor Data[J]. Chinese Journal of Aeronautics, 2011(01)

[11] MENG Tao, WANG Hao, JIN Zhong-he, HAN Ke. Attitude stabilization of a pico-satellite by momentum wheel and magnetic coils[J]. Journal of Zhejiang University (Science A:An International Applied Physics & Engineering Journal), 2009(11)

[12] C. Sabol, R. Burns, and C. McLaughlin. Satellite Formation Flying Design and Evolution. Journal of Spacecraft and Rockets, Vol. 38, No. 2:270–278, March-April 2001.

[13] Zhang Yulin. Theory and Application of Distributed Satellite System[M]. Science Press, 2008.

[14] W. H. Clohessy and R. S. Wiltshire. Terminal Guidance System for Satellite Rendezvous. Journal of the Aerospace Sciences, pages 653–658, 1960.

[15] Starin S R, Yedavalli R K, Sparks A G. Spacecraft formation flying maneuvers using linear quadratic regulation with no radial axis inputs[C]//AIAA Guidance, Navigation, and Control Conference and Exhibit. 2001: 6-9.

[16] Lovell T A, Tragesser S G. Near‐Optimal Reconfiguration and Maintenance of

Close Spacecraft Formations[J]. Annals of the New York Academy of Sciences, 2004, 1017(1): 158-176.

[17] Vaddi S S, Alfriend K T, Vadali S R, et al. Formation establishment and reconfiguration using impulsive control[J]. Journal of Guidance, Control, and Dynamics, 2005, 28(2): 262-268.